Peer-reviewed version available at Catalysts 2018, 8, 279; doi:10.3390/catal8070279

Article

Kinetics of highly active TiO_2 microspheres formation in a presence of ethylammonium nitrate ionic liquid

Anna Gołąbiewska[1], Micaela Checa-Suárez[1,2], Marta Paszkiewicz-Gawron[1], Wojciech Lisowski[3], Edyta Raczuk[1], Tomasz Klimczuk[4], Żaneta Polkowska[5], Ewelina Grabowska[1], Adriana Zaleska-Medynska[1], Justyna Łuczak[6]*

[1] Faculty of Chemistry, University of Gdansk, 80-308 Gdansk, Poland
[2] Faculty of Civil and Environmental Engineering, Escuela Politécnica Nacional, Ecuador
[3] Institute of Physical Chemistry, Polish Academy of Sciences, 01-224 Warsaw, Poland
[4] Faculty of Applied Physics and Mathematics, Gdansk University of Technology, 80-233 Gdansk, Poland
[5] Department of Analytical Chemistry, Faculty of Chemistry, Gdansk University of Technology, 80-233 Gdańsk, Poland
[6] Department of Chemical Technology, Faculty of Chemistry, Gdansk University of Technology, 80-233 Gdansk, Poland
* Correspondence: justyna.luczak@pg.gda.pl; Tel.: +48 58 347-13-65

Abstract: Spherical microparticles of TiO_2 were synthesized by the ionic liquid-assisted solvothermal method at different reaction time (3, 6, 12 and 24h). The properties of the prepared photocatalysts were investigated by means of UV-vis diffuse-reflectance spectroscopy (DRS), BET surface area measurements, scanning electron microscopy (SEM), X-ray diffraction analysis (XRD), and X-ray photoelectron spectroscopy (XPS). The results indicated that the efficiency of phenol degradation was related with a time of the solvothermal synthesis as determined for TiO_2_EAN(1:1)_24h sample. Microparticles of TiO_2_EAN(1:1)_3h formed during the only 3h of synthesis time revealed really high photoactivity under visible irradiation – 75%. This value increased to 80% and 82% after 12h and 24h, respectively. The photoactivity increase was accompanied by the increase of the specific surface area thus pores size, as well as ability to absorb UV-vis irradiation. The high efficiency of phenol degradation of IL-TiO_2 photocatalysts was ascribed to the interaction between the surface of TiO_2 and ionic liquid components (carbon and nitrogen).

Keywords: ionic liquids, ionic liquid-assisted solvothermal reaction, reaction time, titanium dioxide, heterogeneous photocatalysis, visible light

1. Introduction

A worth-mentioning number of recent studies explores photosensitized titanium dioxide photocatalysts' applications inter alia in solar cells, energy storage, hydrogen production via water-splitting process, photocatalytic degradation of organic pollutants for water/air purification [1-5]. Expected low-exploitation costs, prevalence in utility and safety creates motivation for intensified research in the field of solar to chemical energy conversion. Photoactive performance of the pristine TiO_2 nano- and microparticles is limited by its 3.2eV bandgap to the absorption of UV light. Since UV light range constitutes the total radiant energy in only as diminutive amount as 5%, harvesting greater range of solar spectrum is considered vital for achieving significant effectiveness of photocatalysis [5, 6]. Extension of the TiO_2 spectral response range to absorb photons under visible (43%) or/and near infrared (49% of solar spectrum energy) irradiation is crucial for this purpose. The TiO_2 photocatalytic properties can be controlled and its optical response expanded to absorb photons under visible or/and near infrared light irradiation by alteration of the TiO_2 bandgap via morphology engineering [7-10].

It was found that, after excitation, electrons and holes propagate to the nano- and microparticles surface, where they react with electron acceptors and donors, respectively [6, 9, 11, 12]. Additionally, it is noted that slower recombination rate and larger surface area account for more active adsorption/desorption reactions and surface transfer of photoexcited electrons [9, 12, 13], whereas the potential adverse effects that originate in highly defective site, typically developing with the growth of large surface area, may be rectified by higher crystallization of the particles [9].

Ionic liquids (ILs) gain increasing attention in terms of their assistance in TiO_2 synthesis as solvents and spatial and, perhaps, band structuring agents. Their high viscosity, dielectric constant, thus polarity and dispersal capacity are widely recognized as the properties responsible for the charge, steric, and viscous stabilization of small-sized slow-growing crystallites and hindrance of disadvantageous for photocatalytic activity particles aggregation and agglomeration processes [7, 10, 11, 14-23].

The synthesized in a presence of ILs nano- and microparticles are characterized by larger specific surface area, higher crystallization level and less crystalline defects [17]. Hence, in the assistance of ILs, formation of particles of beneficial surface reactivity is promoted, inducing more effective photons absorption, trapping and their migration to the surface. Moreover, energetically simplified pathway of excited electrons through an ionic liquid's HOMO and LUMO orbitals [16], along with prolonged stabilized charge separation is revealed to result in formation of greater amount of reactive oxygen species (ROS) in the subsequent reaction of electrons and holes with oxygen and water, respectively. The generated reactive oxygen species ($^{\bullet}OH$ and $O_2^{\bullet-}$) are crucial reagents in photodegradation of pollutants [16, 17, 24].

Notwithstanding, direct relation between the structure of ILs and size/morphology of nano- and microparticles of semiconductors, such as the TiO_2 photocatalysts, remains still ambiguous. Up till now, the following factors had been reported predominant in effectuating the structure, thus activity of said particles: (1) IL anion type (the number of atoms it is composed of, as well as its steric structure); (2) IL cation type (increasing length of alkyl substituents extends hindrance of particle growth; apart from this, π-π stacking of imidazolium cations promotes ILs role as templating agents); (3) cation – anion interaction energy – the frailer, the weaker cation-anion interactions, the firmer capping on growing TiO_2 particles and the more efficient inhibition/hampering of the unfavorable Ostwald ripening process; (4) type of overall interactions (π-π, van der Waals, Coulomb and electrostatic forces, hydrogen bonding) [15, 16, 21, 25].

Furthermore, the proposed *fons et orgio* of influences on TiO_2 photoactivity are tenable: (1) doping with N, C, F elements after ILs thermal decomposition; (2) directly sensitizing the TiO_2 particles; (3) affecting the transfer of photo-generated charges through the bulk of particles; (4) favoring oxygen vacancies and Ti^{3+} species formation during synthesis [26-28]. However, up to date kinetics of formation of TiO_2 particles during ionic liquid-assisted synthesis was not presented and discussed.

In this regard, in this study, TiO_2 particles had been synthesized solvothermally with the assistance of selected ionic liquid – ethylammonium nitrate [EAN][NO_3], one of the earliest reported in the literature protic ionic liquid [29, 30].

Apart from prevailing in studies topics of synthesis process and characterization of IL-assisted TiO_2 microparticles [22, 30-32], we focused on evaluating functional properties of obtained microparticles, namely – their photoactivity. Alongside the stated, we strive to infer the mechanisms of ILs assistance through exploration of influence of selected ILs, illustrated with the example of ethylammonium nitrate [EAN][NO_3] [29].

We place an emphasis on the essentiality of (1) researching Vis-light induced photoactivity – in comparison to already researched UV-induced photoactivity [19, 25, 33-35] and (2) conducting research in the presence of a model pollutant (2a) neutral in terms of photosensitization of TiO_2, (2b) proposing simple in its mechanism of degradation and mineralization and (2c) of low photoabsorption coefficient [27, 36, 37] – in contrast to common choice of organic dyes (methylene blue, methyl orange, rhodamine B) [7, 10, 13, 18, 19, 25, 38, 39], we applied phenol. What also is

imperative, we excluded the minor in facilitating the photocatalysis reaction active species, while exposing the substantial ones – through active species scavenger tests.

In this article, we present the results of previously non-analyzed and non-reviewed comprehensively [EAN][NO_3]-assisted TiO_2 microparticles, which photocatalytic effect on degradation and mineralization of phenol in aqueous solution vastly exceeded our expectations, reaching as high as 82% of degradation rate in our tests, which are described below. Moreover for the first time we have examined kinetics of TiO_2 microspheres formation in a presence of ethylammonium nitrite ionic liquid.

2. Results

First of all, a set of samples with selected IL to TBOT molar ratios were synthesized and characterized taking into account surface area and photoactivity. Sample labeling, the amount of ILs to precursor used during the preparation procedure, as well as the specific surface area, pore volume of the obtained photocatalysts and their photocatalytic activity under Vis irradiation are given in Table 1. On the basis of the photocatalytic effect we have chosen the sample with the highest activity to examine the kinetics of the TiO_2 microspheres formation in a presence of ethylammonium nitrite ionic liquid, which is showed in Figure 1. As presented in Table 1, the effect of solvothermal synthesis duration (3, 6, 12 and 24h) on surface properties and photoactivity for IL:TBOT ratio equaled to 1:1 was also investigated.

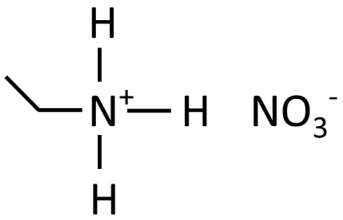

Figure 1. The structure of ethylammonium nitrite [EAN][NO_3] ionic liquid.

2.1. The BET surface area and SEM analysis

The results listed in Table 1 revealed the influence of the ionic liquid content on the specific surface area and pore volume of the synthesized samples. All the samples presented higher specific surface area in comparison with TiO_2 synthesized without IL (184 $m^2.g^{-1}$), and also than that reported for commercially available P25 (50 $m^2.g^{-1}$)[40]. The values of the specific surface area for TiO_2 prepared in a presence of [EAN][NO_3] ranged from 190 $m^2 \cdot g^{-1}$ (sample prepared with the lowest IL:TBOT molar ratio - 1:10) to 233 $m^2 \cdot g^{-1}$ for the sample obtained with IL:TBOT molar ratio of 1:2. In this regard, the direct relation between the amount of the IL in the reaction mixture and the specific surface area for these photocatalysts was detected. However, further increase of the IL content taken to synthesis (up to IL:TBOT molar ratio of 1:1) resulted in a decrease of the pore volume, thereby specific surface area due to probably overloading of the TiO_2 surface with organic salt. It might indicate that IL work like designer agent of microstructures' physical and structural properties.

The scanning electron microscopy images of the pure TiO_2 and IL-assisted TiO_2 particles obtained for various molar ratios of IL:TBOT in a presence of [EAN][NO_3] are presented in Figure 2. The pristine TiO_2 exhibited smooth surface with average size from 0,5-4 μm. In the case of IL-TiO_2 samples it is showed that the sample with the molar ration 1:1 and the sample with a low amount of IL (1:8) present a spherical structure and did not change in relation to pristine TiO_2.

Peer-reviewed version available at Catalysts 2018, 8, 279; doi:10.3390/catal8070279

136 **Table 1.** Characteristics of TiO_2 particles obtained by [EAN][NO_3] – assisted solvothermal synthesis.

Sample	Time of the synthesis	Molar ratio (IL:TBOT)	Specific surface area ($m^2.g^{-1}$)	Pore volume ($cm^3.g^{-1}$)	Phenol degradation efficiency under 60 min of Vis irradiation (%)	Rate of phenol degradation under visible light (λ> 420) [$\mu mol \cdot dm^{-3} \cdot min^{-1}$]
TiO_2_pristine	24	-	184	0.069	7	0.18
TiO_2_EAN(1:10)_24h	24	1:10	190	0.093	28	1.01
TiO_2_EAN(1:8)_24h	24	1:8	211	0.102	19	0.55
TiO_2_EAN(1:5)_24h	24	1:5	216	0.105	33	1.11
TiO_2_EAN(1:3)_24h	24	1:3	216	0.105	36	1.17
TiO_2_EAN(1:2)_24h	24	1:2	233	0.113	41	1.32
TiO_2_EAN(1:1)_24h	24	1:1	221	0.108	82	3.12
TiO_2_EAN(1:1)_3h	3	1:1	239	0.12	75	2.28
TiO_2_EAN(1:1)_6h	6	1:1	207	0.101	75	2.38
TiO_2_EAN(1:1)_12h	12	1:1	209	0.102	80	2.53

137

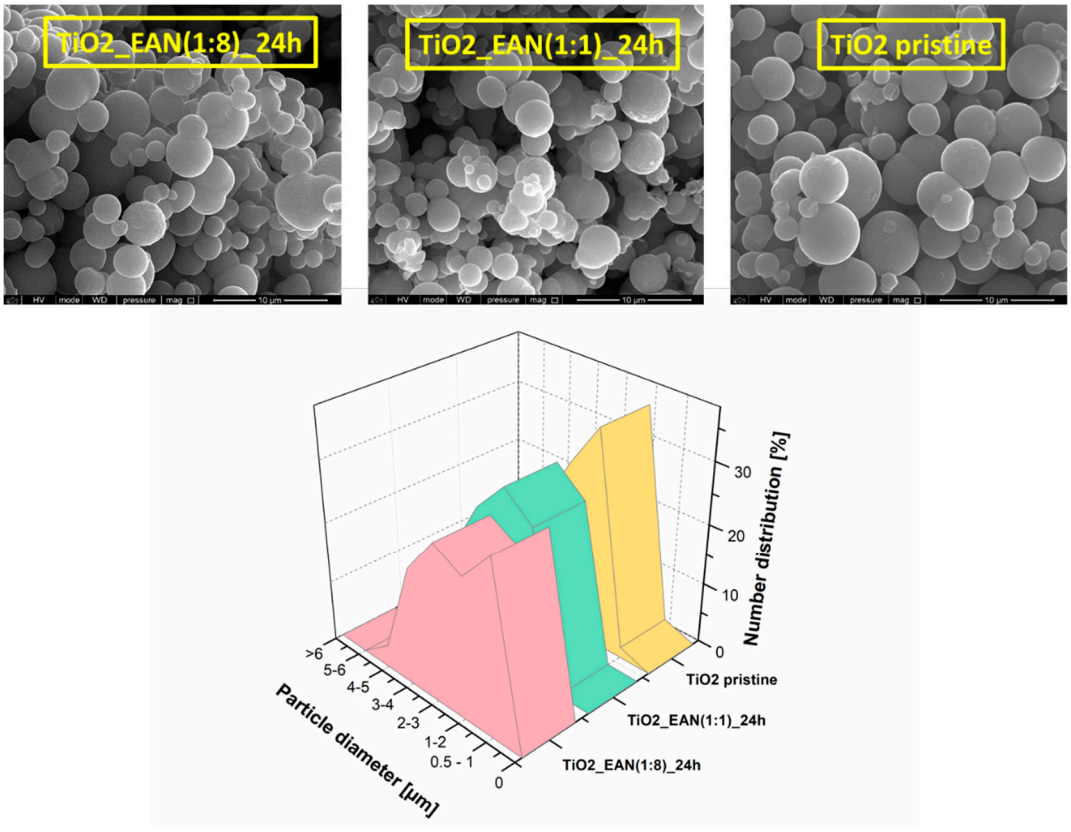

138

139 **Figure 2.** SEM images of TiO_2 obtained from IL-assisted solvothermal synthesis: TiO_2_EAN(1:8)_24h;
140 TiO_2_EAN(1:1)_24h and reference TiO_2.

The experiments of the TiO_2_EAN(1:1)_24h sample preparation performed in the different time regimes revealed that 3h of the solvothermal synthesis is enough to obtain the TiO_2 microspheres (see SEM images presented in Figure 3 below). However, the reaction yield was relatively low (only 19%) and increased with increasing reaction time (38% for 6h, 65% for 12h and 93% for 24h). Moreover, elongation of the synthesis time resulted at first in decrease of the specific surface area from 239 $m^2.g^{-1}$ (after 3h) to 207 $m^2.g^{-1}$ (after 6h), and then in the enlargement of the specific surface area to 221 $m^2.g^{-1}$ (after 24h).

Explanation of this observation may be found in SEM images of microparticles prepared with the same amount of substrates (molar ratio of TBOT to ILs equaling to 1:1), however differing by the time of thermal treatment (3, 6, 12 and 24 hours) presented in Figure 3. In all the introduced variations, the majority of the particles lie within the scope of 1-3 μm for 3h (48%), 2-3μm for 6 (24%) and 24 hours (28%), and 3-4 μm for 12 hours (19%). Percentage contribution of the particles with diameter above 4 μm was rarely reached and never exceeds 15% for all the obtained samples. In the images sequence presented below, we noted that sample subjected to thermal treatment for 3 h is mainly composed of a large number of small spherical particles with a range of 1-3 μm. Nonetheless, between particles synthesized in 6, 12- and 24-hour regime, less of a difference was recognized. In this regard, high surface area of the particles prepared within 3h may be related to higher contribution of the smallest particles.

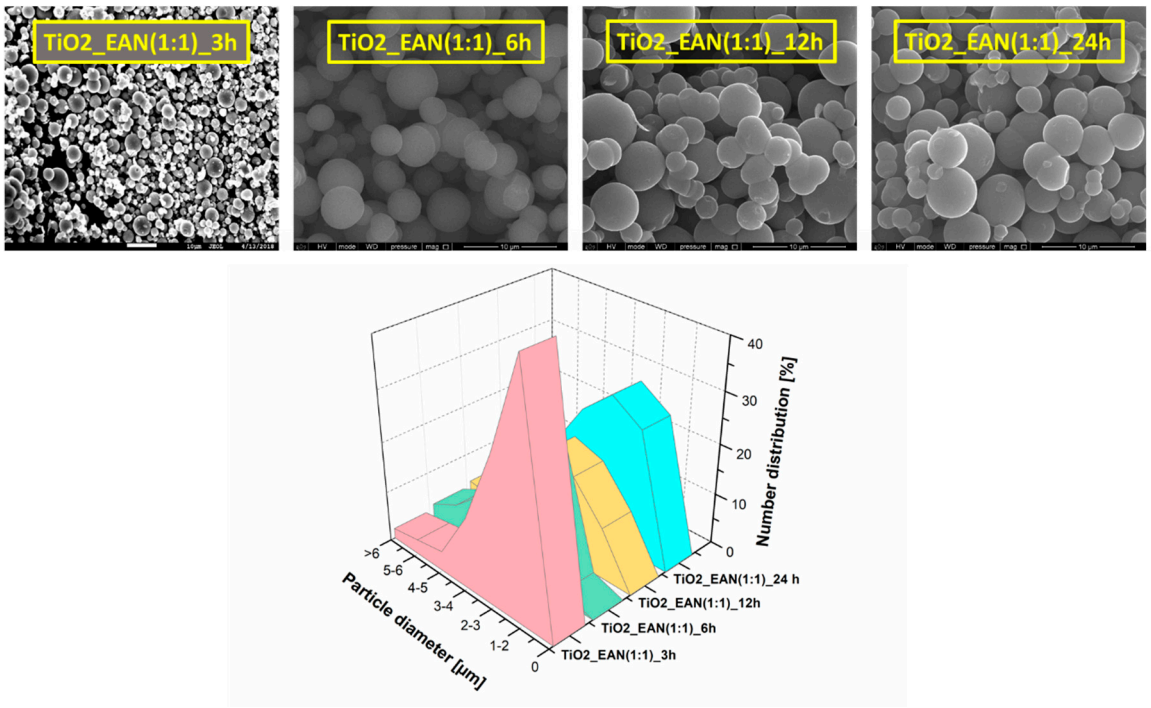

Figure 3. SEM images of TiO2_EAN(1:1) obtained in different synthesis time: 3h, 6h, 12h and 24h.

2.2. XRD analysis

PXRD patterns for the series of TiO_2_EAN are presented in Figure 4-5 All patterns looked similar since the samples contained only the anatase (TiO_2) phase. The open circles represent experimental data points, a solid red line is a profile fitting (LeBail method) and vertical bars mark positions of the expected Bragg reflections for the used model (I 41/a m d, s.g. # 141). The LeBail fit given lattice parameters for TiO_2 that are gathered in Table 2. The lattice parameters are similar and are close to reported by I. Djerdj and A.M. Tonejc [41]. The PXRD reflections are broad which indicates small crystallite size that was estimated to be between 5,0 and 6,5 nm. However, no correlation was observed between the amount of ionic liquid taken for synthesis as well as preparation time and the crystallite size.

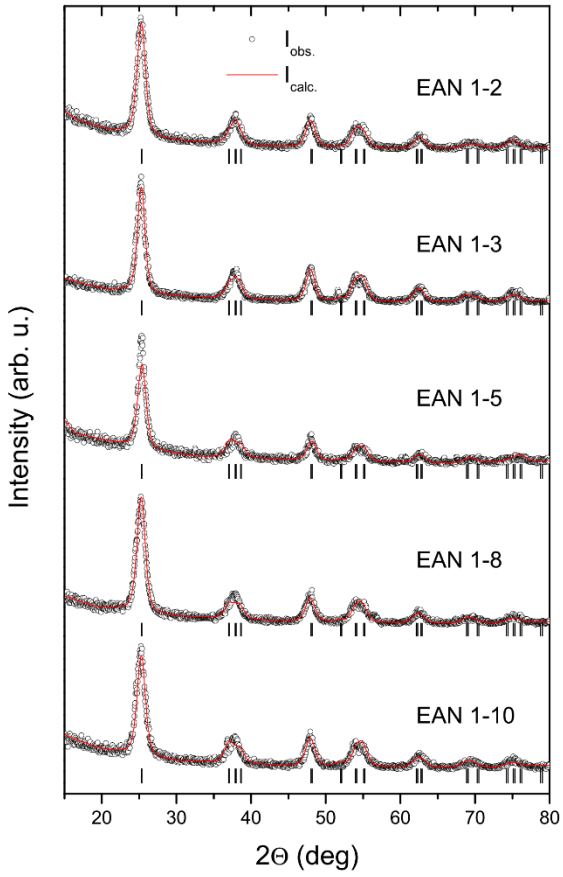

171

172 **Figure 4.** XRD pattern of TiO_2-EAN prepared with different IL-TBOT molar ratio. A solid line is
173 a profile fit to the experimental data (open circles). A Bragg reflections are marked by vertical bars.

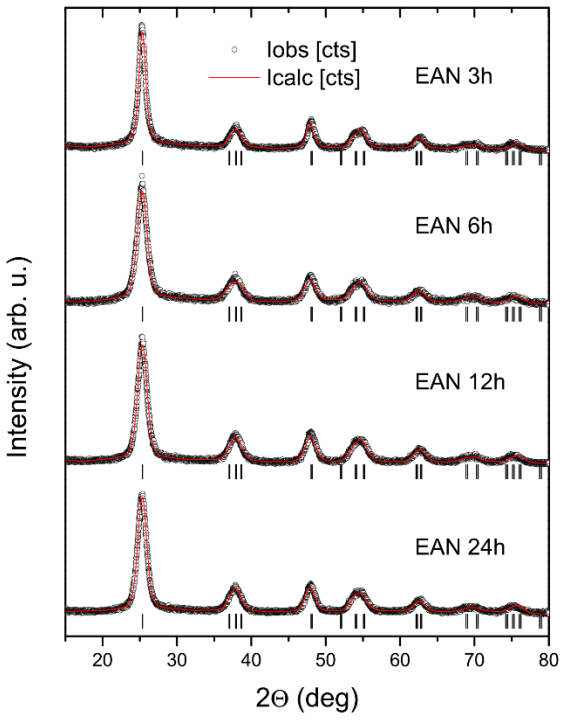

174

175 **Figure 5.** XRD pattern of TiO_2_EAN prepared with IL-TBOT molar ratio of 1:1 synthesized at different
176 synthesis times. A solid line is a profile fit to the experimental data (open circles). A Bragg reflections
177 are marked by vertical bars.

Peer-reviewed version available at Catalysts 2018, 8, 279; doi:10.3390/catal8070279

178 **Table 2.** Lattice parameters and average crystallite size of the TiO_2_EAN photocatalysts.

Sample	a (Å)	c (Å)	d (Å)
TiO_2_EAN(1:1)_3h	3.8051(3)	9.554(2)	65
TiO_2_EAN(1:1)_6h	3.7907(7)	9.504(3)	50
TiO_2_EAN(1:1)_12h	3.7892(6)	9.507(3)	55
TiO_2_EAN(1:1)_24h	3.7890(6)	9.502(3)	60
TiO_2_EAN(1:2)_24h	3.7899(7)	9.499(3)	55
TiO_2_EAN(1:3) _24h	3.7926(8)	9.506(4)	60
TiO_2_EAN(1:5) _24h	3.7814(11)	9.472(6)	65
TiO_2_EAN(1:8) _24h	3.7953(9)	9.483(5)	55
TiO_2_EAN(1:10) _24h	3.7942(12)	9.476(7)	55

179

180 *2.3. XPS analysis*

181 The elemental surface composition of the selected ILs-TiO_2 specimens, evaluated by XPS, is
182 shown in Table 3. The titanium, oxygen, carbon and nitrogen were detected and the
183 corresponding high-resolution (HR) XPS spectra of Ti 2p, O 1s, C 1s and N 1s are presented in
184 Figure 6. The chemical character of elements is identified in the deconvoluted spectra in Figure
185 6 and Table 3. The Ti 2p, O 1s and C 1s spectra exhibit features, characteristic for the ILs-TiO_2
186 specimens [16, 42]. The N 1s signal at 400 eV is commonly interpreted as the surface C-N bond.
187 Only for the TiO_2_EAN(1:1) sample thermally treated for 24 h, the additional signal appears at
188 about 402.8 eV, which may be assigned to oxidized nitrogen surface species.

189 The XPS data collected in Table 4 revealed the surface chemical composition of the
190 TiO_2_EAN(1:1)_24h samples to be different than the sample of lower amount of
191 TiO_2_EAN(1:8)_24h. For the last one the contribution of the $Ti^{(3+)}$ fraction is about 30% smaller
192 and the nitrogen amount is evidently lower than for TiO_2_EAN(1:1)_24h sample. These
193 observations confirmed higher amount of IL on the TiO_2_EAN(1:1)_24h sample surface
194 (analogous relation was observed also for carbon atom). In the series of TiO_2_EAN(1:1) samples,
195 differing by the time of thermal treatment, we noted systematic decrease of the oxygen Ti-O_{surf}
196 fraction with increasing time of thermal treatment from 6 h to 24 h and significantly smaller
197 surface concentration of nitrogen for 24-hour synthesized sample (Table 4). Moreover, for the
198 last sample the oxidised form of nitrogen species appears in addition to the main nitrogen N-C
199 surface fraction (Figure 6). These observations indicated the surface transformation of IL-
200 assisted TiO_2 in prolonged time of thermal treatment.

201 To elucidate the effect of phenol-degradation processing on the chemical composition of
202 TiO_2_EAN photocatalyst, we analyzed both the sample after 3-cycles of photocatalytic
203 processing and the same sample washed with deionized water. The results are compared in
204 Figure 6 and Table 3. One can see nitrogen atoms concentration is similar for both samples.
205 However, the water washed sample exhibits significantly larger surface amount of titanium
206 faction $Ti^{(3+)}$ and relatively higher contribution of -OH surface species (see O 1s and C 1s fractions
207 in Table 3).

208

209

Peer-reviewed version available at Catalysts 2018, 8, 279; doi:10.3390/catal8070279

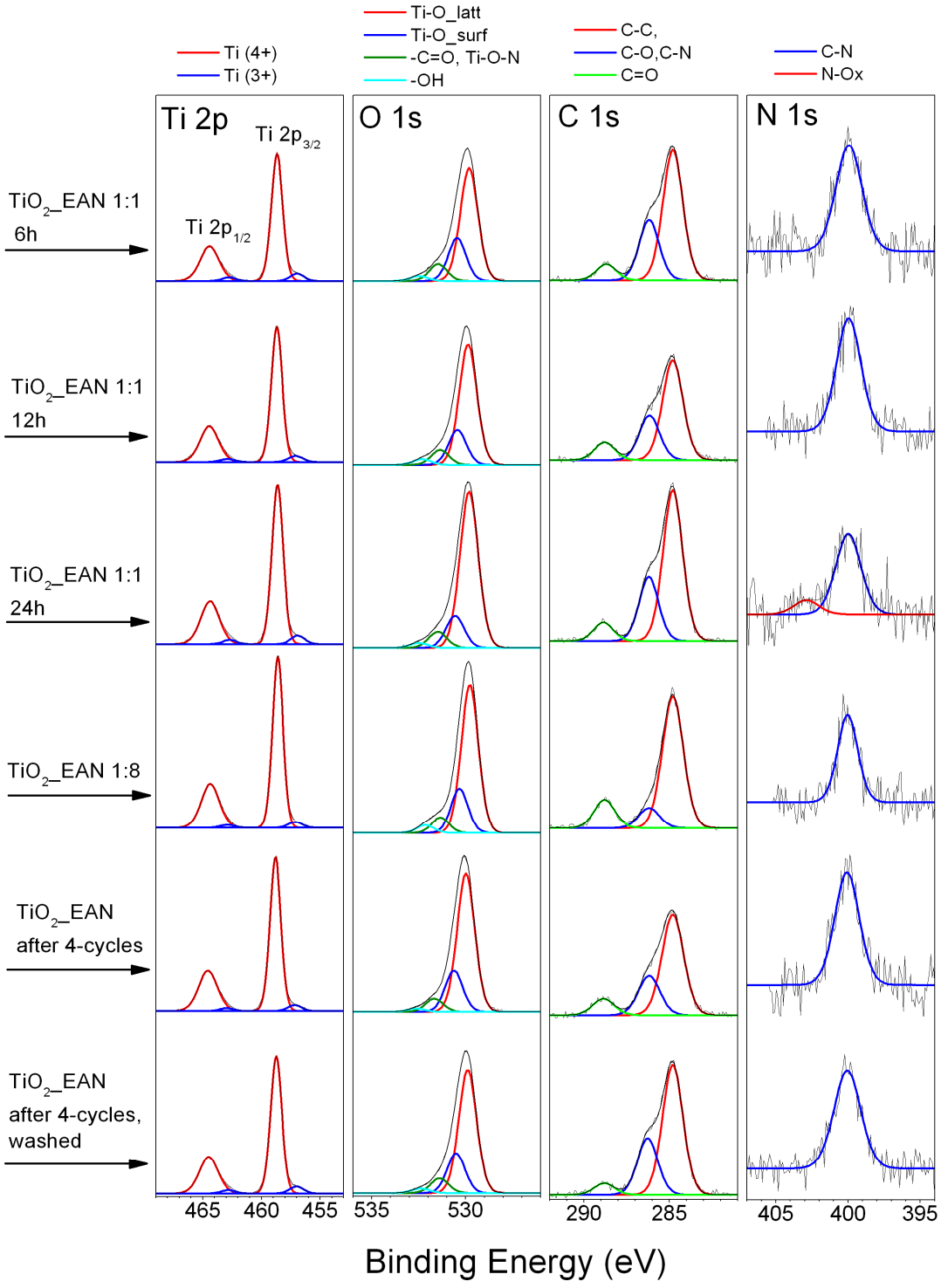

Figure 6. High resolution XPS spectra of elements detected in the surface layer of [EAN][NO_3]-modified TiO_2 particles.

Table 3. Elemental composition (in at. %) and chemical character of titanium, oxygen, carbon and nitrogen states in the surface layer of [EAN][NO_3]-modified TiO_2 particles, evaluated by XPS analysis.

Sample label		Ti 2p$_{3/2}$ fraction (%)			O1s fraction (%)					C1s fraction (%)				N1s fraction (%)	
	∑ Ti (at.%)	Ti(4+) 458.7±0.1 eV	Ti(3+) 457.0±0.1 eV	∑ O (at.%)	Ti-O$_{latt}$ 529.9±0.1 eV	Ti-O$_{surf}$ 530.5±0.1 eV	- Ti-O-N, -C=O 531.5±0.1 eV	-OH 532.4±0.1 eV	∑ C (at.%)	"A" C-C 284.8 eV	"B" C-OH, C-N 286.2±0.1 eV	"C" -C=O, 288.9±0.1 eV	∑ N (at.%)	N-C 399.9 ±0.1 eV	N-Ox 402.8 ±0.1 eV
TiO_2_EAN 1:1_6h	23.15	93.37	6.63	61.97	63.55	24.13	9.54	2.78	14.35	63.03	29.19	7.78	0.53	100	0
TiO_2_EAN 1:1_12h	24.00	94.06	5.94	63.51	68.33	19.89	8.50	3.28	11.94	61.53	27.49	10.99	0.54	100	0
TiO_2_EAN 1:1_24h	23.37	93.64	6.36	63.00	74.56	15.33	7.72	2.39	13.24	64.56	27.42	8.02	0.38	84.89	5.11
TiO_2_EAN 1:8_24h	24.32	95.44	4.56	63.80	68.52	20.58	7.25	3.65	11.61	73.05	11.18	15.77	0.29	100	0
TiO_2_EAN _4-cycles	24.61	94.47	4.78	63.77	70.46	21.06	6.75	1.73	11.14	64.12	25.22	10.66	0.49	100	0
TiO_2_EAN _4-cycles (washed)	23.53	93.10	6.13	62.35	67.42	21.84	8.15	2.59	13.64	65.63	28.52	5.84	0.48	100	0

2.4. UV-Vis spectrum

The UV-vis adsorption spectra of TiO_2 synthesized with various molar ratio of [EAN][NO_3] to TBOT are presented in Figure 7. Pristine TiO_2 is only photoactive under the UV region (λ<400 nm). The addition of the ionic liquid to the TiO_2 synthesis environment increased the absorption range of IL-TiO2 being noticeably photoactive at above 420 nm. The absorption properties of the samples prepared with IL were superior in comparison with pristine TiO_2 in the visible light range, whereas all samples showed similar UV absorption. Generally, higher IL amount used for synthesis resulted in the enhancement of the Vis light absorption by the IL-TiO_2 photocatalysts.

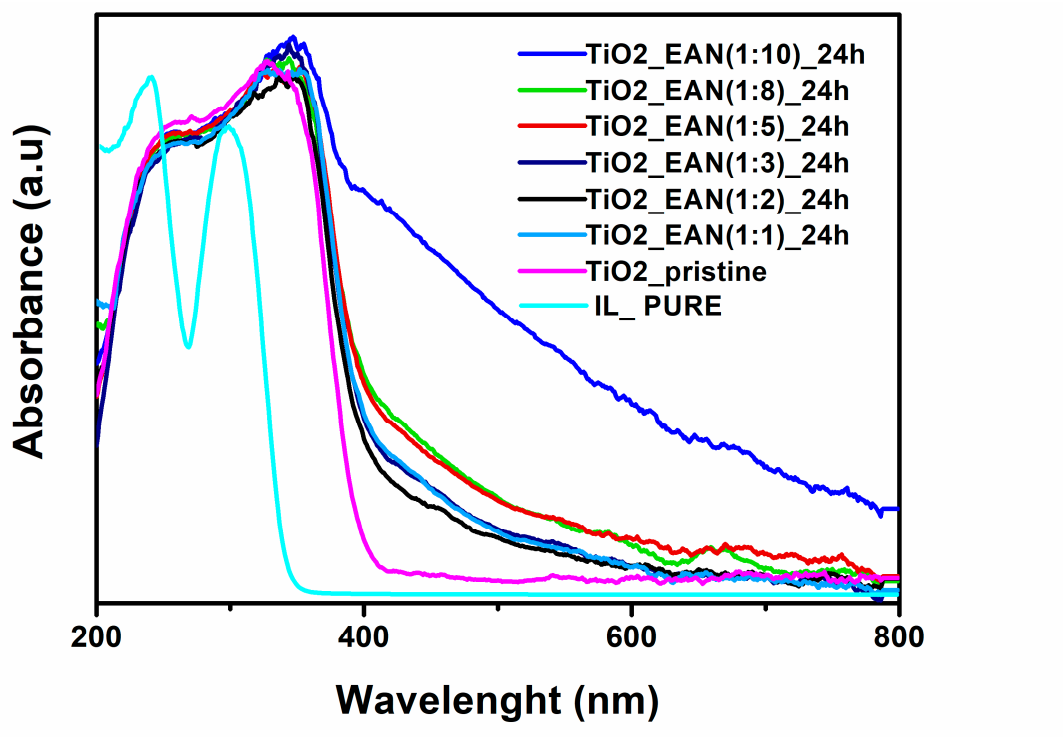

Figure 7. UV-vis adsorption spectra of TiO_2 synthesized using various molar ratio of [EAN][NO_3] to TBOT..

Interesting results were also obtained for the experiments where the influence of the reaction time was taken into account (Figure 8). When increasing the reaction time the enhancement of visible light absorption by IL-TiO_2 was observed. Thereby, the sample prepared during 24h was characterized by the significantly broader absorption and the highest red shift of the absorption edge, thereby higher effectiveness to create electron–hole pairs.

2.5. Photocatalytic activity of IL-TiO2 in phenol decomposition model reaction

The photocatalytic activity of the IL-TiO_2 samples was evaluated by the degradation of phenol model compound under visible light (λ>420 nm) irradiation. The obtained results are summarized in Table 1 and presented in Figure 9. As it was mentioned above, before illumination, the solution was stirred for 30 min in the dark to establish molecular adsorption equilibrium. Pristine TiO_2 synthesized by the solvothermal method without addition of the ionic liquid was used as the reference sample.

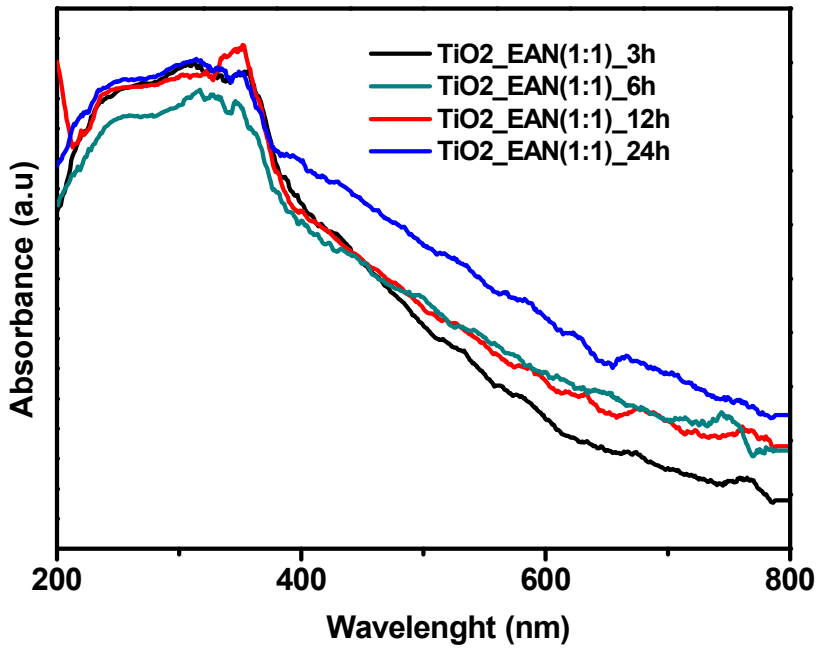

Figure 8. UV-vis adsorption spectra of TiO_2_EAN(1:1) photocatalyst prepared in 3, 6,12 and 24h.

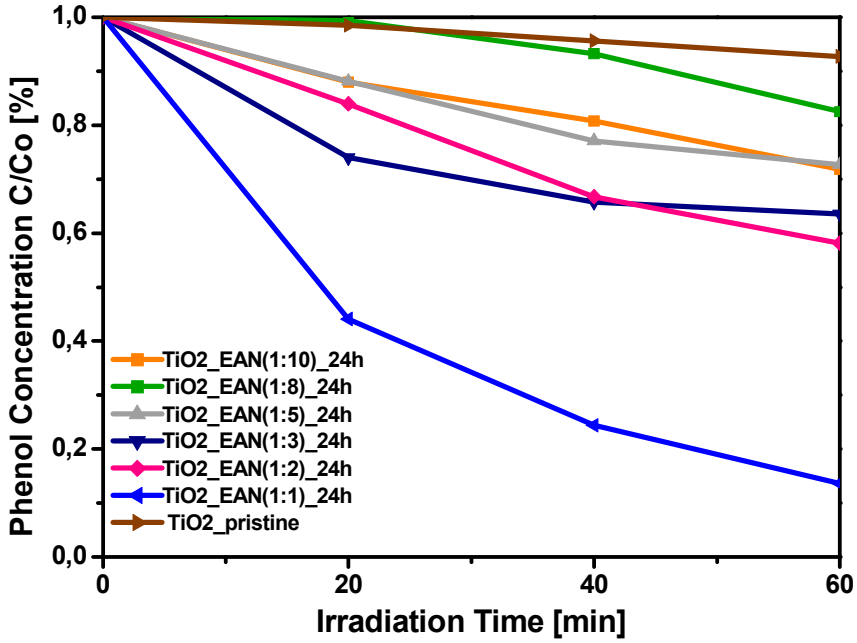

Figure 9. Efficiency of phenol degradation under visible light (λ>420 nm) in a presence of TiO2 prepared in [EAN][NO_3].

It was found that the TiO_2_EAN microparticles exhibited higher photoefficiency than pristine TiO_2, which is consistent also with higher BET specific surface areas and enhanced optical properties. After 60 min of photocatalytic process, 7% of phenol was degraded using unmodified TiO_2, however the TiO_2_EAN efficiency was higher and strongly influenced by the amount of ILs used during the synthesis. For example, up to 82% of phenol was degraded in the presence of photocatalyst TiO_2_EAN(1:1)_24h, where molar ratio of [EAN][NO_3] to TBOT taken for synthesis was 1:1. This value is about 5.5 times higher compared to pristine TiO_2, indicating its excellent photocatalytic activity. This observation was correlated with the UV-vis adsorption spectra, where TiO_2_EAN(1:1)_24h sample showed the highest extension of the absorption edge to the visible light region. It was found that the samples prepared with IL:TBOT molar ratio 1:10

and 1:8 revealed the lowest photoactivity among the photocatalysts obtained in the presence of ethylammonium nitrate IL. In this regard, the photodegradation efficiency increased with increasing the quantity of ionic liquid taken to synthesis (thereby IL present at the TiO_2 surface).

Moreover, the efficiency of phenol degradation was also related with time of the solvothermal synthesis as determined for TiO2_EAN(1:1) sample. Microparticles of TiO_2_EAN(1:1)_3h formed during only 3h of synthesis time revealed really high photoactivity under visible irradiation – 75%. This value increased to 80% and 82% after 12h and 24h, respectively. The photoactivity increase was accompanied by increase of the specific surface area thus pore sizes as well as ability to absorb UV-vis irradiation. Additionally, based on the XPS measurements it was concluded that the increase in the visible light absorption and the enhancement of the photocatalytic activity may be related to the highest quantity of carbon and $Ti^{(+3)}$ defects at the TiO_2 surface.

To investigate the degradation/regeneration capacity and the structural stability during the entire process, we performed the stability tests for the sample characterized by the best photocatalytic activity under Vis light irradiation. In the stability tests, the same sample was repeatedly used in the phenol photodegradation reaction for 3 times. As shown in Figure 10, the significant drop of the phenol removals from 84% to 33% was found.

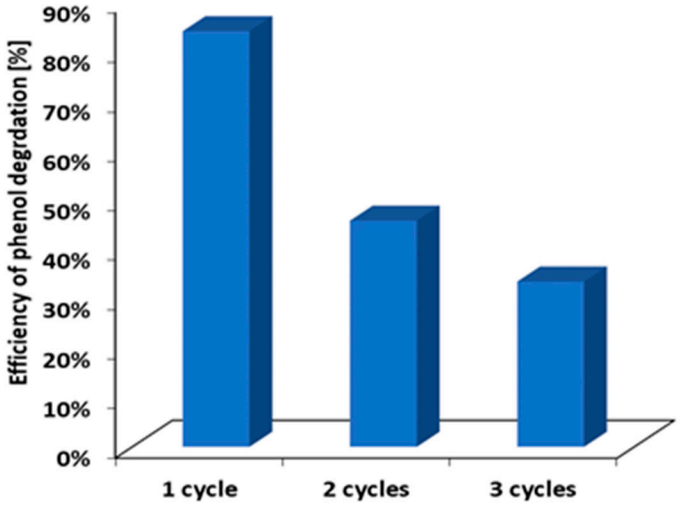

Figure 10. Phenol removals in the photodegradation using the TiO_2 microspheres in a cycled mode.

In order to further clarify the possible mechanism of phenol degradation, reactive species trapping tests were designed. Controlled photoactivity experiments using different radical scavengers (ammonium oxalate as scavenger for h^+, $AgNO_3$ as scavenger for e^-, benzoquinone as scavenger for $O_2^{\bullet-}$ radical species, and tert-butyl alcohol as scavenger for $^{\bullet}OH$ species) were carried out similarly to the above described photocatalytic degradation process. The only exception was that the radical scavengers were added to the reaction system. The addition of ammonium oxalate and $AgNO_3$ had weak inhibition efficiency of phenol degradation, indicating that h^+ and e^- had negligibly small effect on the mechanism of photocatalytic degradation. The photocatalytic conversion falls by approximately half when the tert-butyl alcohol (TBA) as the scavenger for hydroxyl radicals was used. As shown in Table 4 when benzoquinone as the trapping agent of $O_2^{\bullet-}$ was added into phenol solution under visible irradiation the photodegradation of phenol significantly declined to about 7%. These results clearly suggested that the photocatalytic degradation of phenol under Vis irradiation in the presence of TiO_2_EAN(1:1) was mainly intimate with the photogenerated superoxide radical species. Secondly, the photogenerated OH radicals were also involved in the decomposition of phenol.

Preprints (www.preprints.org) | NOT PEER-REVIEWED | Posted: 15 May 2018 doi:10.20944/preprints201805.0216.v1

Peer-reviewed version available at Catalysts 2018, 8, 279; doi:10.3390/catal8070279

Table 4. Effect of scavengers' addition on phenol degradation efficiency under Vis irradiation.

TiO_2_EAN(1:1)_24h	Efficiency of phenol degradation (%) filter **>420 nm**				
Scavenger type	**benzoquinone**	**$AgNO_3$**	**Tert-butyl alcohol**	**Ammonium oxolate**	**Without scavenger**
Active species	**$O_2^{\cdot-}$**	**e^-**	**OH·**	**h^+**	**-**
Vis >420 nm	6.89	78.94	33.56	81.38	86.35

In order to explain what might have contributed to the increase in the photoactivity of TiO_2_ILs, the decomposition level of ionic liquid cations has been investigated a by using chromatography techniques. It has been demonstrated that the ethylammonium nitrate ionic liquid was degraded in 97% after 24h solvothermal reaction. Therefore, it was probably that TiO_2 could be doped with nitrogen and carbon or/and surface-modified by carbon species. However, based on the XPS analysis, the Ti-N interactions between released nitrogen atoms, resulting from IL's thermal decomposition, and TiO_2 matrix have not been observed. Thus, although we could expect incorporation of nitrogen and carbon atoms in a crystalline lattice of TiO_2, performed analysis did not confirm it. Nevertheless, it should be remembered that due to the low ionic liquid content on the TiO_2 surface, a low level of XPS detection (d.l. = 0.1 at.%) could affect on the results. According to the literature, it could be generally stated that if TiO_2 particles growth in the presence of N and C precursors and under elevated temperature conditions, usually N and C atoms are incorporated into crystal lattice of semiconductors [43-45].

In order to identify the origin of visible light – induced activity, phenol degradation rate was plotted depending on the surface area values as well as carbon and nitrogen content in the surface layer. Data presented in Figure 11 suggested that the observed increase in photoactivity could be most interpreted by presence of nitrogen in the surface layer. Although the origin of photoactivity is not clear at this moment, it is crucial to note that preparation of highly active TiO_2 spheres was developed.

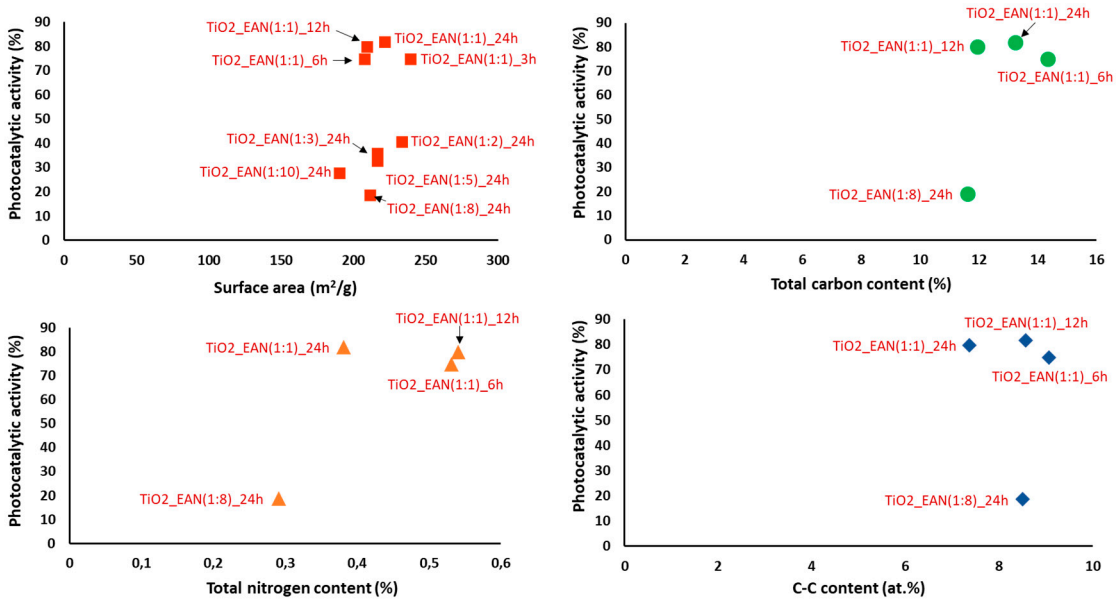

Figure 11. Dependence the (a) surface area, (b) total carbon content, (c) C-C content and total nitrogen content on the photocatalytic activity.

3. Materials and Methods

3.1. Materials

For the aforementioned synthesis' purpose the following reagents have been applied: (1) titanium(IV) butoxide (TBOT) – as the TiO_2 microparticles direct precursor and (2) 36% hydrochloric acid (HCl) – as a pH stabilizer, sourced from Sigma–Aldrich; (3) anhydrous ethyl alcohol (99.8% ethanol) – as the reaction medium (from POSCH S.A.); (4) ethylammonium nitrate (from IOLITEC, purveyed with ≥97% of purity) – the assisting ionic liquid and (5) deionized water provided locally.

3.2. Preparation of IL-assisted TiO_2 particles

The preparation of TiO_2 microparticles was carried out emulating the method reported in [16], of the following summary: (1) TBOT was dispersed in ethanol through dropwise pouring, under constant vigorous stirring; (2) HCl, deionized water and the due amount of IL – adequate to the applied molar ratio of TBOT to IL – were dissolved under unchanged conditions to the point of attaining a pellucid solution. Afterwards, the ensuing mixture was transferred into an inner Teflon and an outer stainless-steel autoclaves to be incubated at 180°C for 24h (for various TBOT to IL molar ratios) and for 6, 12 and 24h (for 1:1 TBOT to IL molar ratio) for the purpose of kinetics of crystal growth evaluation. Subsequently, the autoclaves were cooled down to the room temperature and obtained precipitate was cleansed through numerous washings with deionized water and ethanol, and then dried at 60°C during 4h. The preparation ended with the 2–hour calcination of plateau at 200°C, that was being reached at the 2°C/min slope. For reference, pristine TiO2 was as-synthetized – with the exception of the IL presence.

3.3. Surface properties characterization

The Brunauer-Emmett-Teller (BET) surface area was calculated by N_2 absorption-desorption isotherms at 77K on a Micromeritics Gemini V200 Shimadzu analyzer (equipped with the VacPrep 061 Degasser). The morphology of TiO_2 microparticles were studied by scanning electron microscopy (SEM) analysis, performed under a Hitachi TM-1000 microscope. The chemistry of the surface was researched by X-Ray photoelectron spectroscopy (XPS), the results were obtained with a PHI 5000 VersaProbeTM(ULVAC-PHI) spectrometer of monochoromatic Al Kα radiation (h=1486.6 eV). Phase purity of the samples was determined by powder X-ray diffraction (PXRD) using a PANalytical X'Pert Plus diffractometer with Cu Kα radiation. To determine the unit cell parameters, profile fits were performed on the powder diffraction data through the use of the HighScore program using Thompson–Cox–Hastings pseudo-Voigt peak shapes. The average crystallite size was calculated using the Scherrer equation.

The decomposition level of ionic liquid cations was analyzed by using Dionex ICS 1100 liquid chromatograph. Deionized water containing 0,21 % (v/v) of methanesulfonic acid (Sigma Aldrich) was used, as a mobile phase. The separation was carried out isocratically with using Dionex ION PAC, CS16 column (3 x 250 mm Dionex) at 35°C. The flow rate was 0.36 mL min^{-1}. Each sample (before and after solvothermal reaction) was measured in triplicate. The decomposition level was calculated as:

$$\eta IL(\%) = 100 \times C_0 - C/C_0$$

where: C_0 – is the initial concentrations of cations of ILs; C – is the concentrations of cations of ILs after the solvothermal reaction.

3.4. Evaluation of photocatalytic activity

The photocatalytic activity was measured through the phenol decomposition rate under visible-light irradiation. For this aim, we dispersed 0.125 g of obtained photocatalyst in the 25 ml of phenol

aqueous solution (C_0 = 25mg/l) inside a cylindrical reactor with a circular quartz window. In use there was a reactor fitted with a cooling jacket, during the reaction cooled by the constant flow of water at ≤10°C, supplied in aeration at 5 dm3/h. The reactor's quartz–windowed side was exposed to illumination of intensity equaling to 3 mW/cm2 (by 1000 W Xenon lamp, 6271H Oriel; optical filter >420 nm, GG 420).

In order to establish the absorption-desorption equilibrium between phenol and photocatalyst prior to the reaction, the suspension was allocated to 30-minutes long stirring in the dark, preliminarily to the photo-initiation of the catalysis. About 1 ml of the suspension was sampled from the reactor, then. During the irradiation – the samples were taken in 3, 20–minute intervals. Each sample was filtered through syringe filters (Ø=0,2 μm) for the removal of photocatalyst microparticles, anterior to the due evaluation. The concentration of the remaining phenol was measured colorimetrically (λmax = 480 nm), after the derivatization with diazo-p-nitroaniline, with UV-Vis spectrometer (Evolution 220, Thermo-Scientific).

5. Conclusions

This study is the first step towards enhancing our understanding of effect of ethylammonium nitrate ionic liquids on surface properties of TiO_2 spheres formed in the solvothermal synthesis. In summary, the TiO_2 microspheres with a superior visible-light photocatalytic activity were prepared in the presence of the ethylammonium nitrate ionic liquid by using a solvothermal method followed by calcination process. It should be highlighted that the most active $_{TiO2}$ samples formed in the presence of [EAN][NO3] possessed almost the same activity induced by visible light than P25 TiO_2 under UV radiation. Phenol degradation rate equaled to 3.12 μmol/dm3/min for TiO_2_EAN/Vis system, while it was 3.46 μmol/dm3/min for P25/UV system. In this paper, kinetics of highly active TiO_2 microspheres formation in a presence of ethylammonium nitrate ionic liquid has been examined. The obtained results revealed that, the microparticles of TiO_2_EAN(1:1)_3h formed during only 3h of synthesis time revealed really high photoactivity under visible irradiation – 75%. This value increased to 80% and 82% after 12h and 24h, respectively. However, the reaction yield for the 3h synthesis time was relatively low (only 19%) and significantly increased with increasing reaction time (38% for 6h, 65% for 12h and 93% for 24h). The photoactivity increase was accompanied by increase of the specific surface area thus pore sizes as well as ability to absorb Vis irradiation.

The effective interactions between ionic liquid components mainly: carbon, nitrogen and microparticles surface of TiO_2 were clearly demonstrated by the XPS analysis. This factor could result in an excellent visible-light photocatalytic activity for the IL-TiO_2 samples prepared. The radicals trapping experiments revealed that $O_2^{\bullet-}$ and $OH^{\bullet}$ were the main active species during the degradation process.

Funding: This research was funded by the National Science Center within the program SONATA 8, research grant: "Influence of the ionic liquid structure on interactions with TiO2 particles in ionic liquid assisted hydrothermal synthesis", contract No. 2014/15/D/ST5/02747.

Author Contributions: Conceptualization, Adriana Zaleska-Medynska and Justyna Łuczak; Funding acquisition, Justyna Łuczak; Investigation, Anna Gołąbiewska, Micaela Checa-Suárez, Marta Paszkiewicz-Gawron, Wojciech Lisowski, Edyta Raczuk, Tomasz Klimczuk, Żaneta Polkowska and Justyna Łuczak; Project administration, Ewelina Grabowska; Supervision, Adriana Zaleska-Medynska and Justyna Łuczak; Writing – original draft, Anna Gołąbiewska, Wojciech Lisowski, Edyta Raczuk, Tomasz Klimczuk, Ewelina Grabowska and Justyna Łuczak; Writing – review & editing, Adriana Zaleska-Medynska and Justyna Łuczak.

Conflicts of Interest: The authors declare no conflict of interest.

References

1. Hoffmann, M. R.; Martin, S. T.; Choi, W.; Bahnemann, D. W., Environmental applications of semiconductor photocatalysis. *Chemical reviews* **1995,** *95* (1), 69-96, 10.1021/cr00033a004.

2. Fujishima, A.; Rao, T. N.; Tryk, D. A., Titanium dioxide photocatalysis. *Journal of Photochemistry and Photobiology C: Photochemistry Reviews* **2000,** *1* (1), 1-21, 10.1016/S1389-5567(00)00002-2.

3. Pelaez, M.; Nolan, N. T.; Pillai, S. C.; Seery, M. K.; Falaras, P.; Kontos, A. G.; Dunlop, P. S. M.; Hamilton, J. W. J.; Byrne, J. A.; O'Shea, K.; Entezari, M. H.; Dionysiou, D. D., A review on the visible light active titanium dioxide photocatalysts for environmental applications. *Applied Catalysis B: Environmental* **2012,** *125*, 331-349, 10.1016/j.apcatb.2012.05.036.

4. Fox, M. A.; Dulay, M. T., Heterogeneous photocatalysis. *Chemical reviews* **1993,** *93* (1), 341-357, 10.1021/cr00017a016.

5. Thompson, T. L.; Yates, J. T., Surface science studies of the photoactivation of TiO_2 new photochemical processes. *Chemical Reviews* **2006,** *106* (10), 4428-4453, 10.1021/cr050172k.

6. Zhang, B.; Xue, Z.; Xue, Y.; Huang, Z.; Li, Z.; Hao, J., Ionic liquid-assisted synthesis of morphology-controlled TiO_2 particles with efficient photocatalytic activity. *RSC Advances* **2015,** *5* (99), 81108-81114, 10.1039/C5RA17213F.

7. Ramanathan, R.; Bansal, V., Ionic liquid mediated synthesis of nitrogen, carbon and fluorine-codoped rutile TiO_2 nanorods for improved UV and visible light photocatalysis. *RSC Advances* **2015,** *5* (2), 1424-1429, 10.1039/C4RA14510K.

8. Xu, H.; Ouyang, S.; Liu, L.; Reunchan, P.; Umezawa, N.; Ye, J., Recent advances in TiO_2-based photocatalysis. *Journal of Materials Chemistry A* **2014,** *2* (32), 12642-12661, 10.1039/C4TA00941J.

9. Zhang, F.; Sun, D.; Yu, C.; Yin, Y.; Dai, H.; Shao, G., A sol–gel route to synthesize SiO_2/TiO_2 well-ordered nanocrystalline mesoporous photocatalysts through ionic liquid control. *New Journal of Chemistry* **2015,** *39* (4), 3065-3070, 10.1039/C4NJ02282C.

10. Alammar, T.; Noei, H.; Wang, Y.; Mudring, A.-V., Mild yet phase-selective preparation of TiO_2 nanoparticles from ionic liquids–a critical study. *Nanoscale* **2013,** *5* (17), 8045-8055, 10.1039/C3NR00824J.

11. Ahmed, E.; Breternitz, J.; Groh, M. F.; Ruck, M., Ionic liquids as crystallisation media for inorganic materials. *CrystEngComm* **2012,** *14* (15), 4874-4885, 10.1039/C2CE25166C.

12. Bhattacharyya, K.; Majeed, J.; Dey, K. K.; Ayyub, P.; Tyagi, A. K.; Bharadwaj, S. R., Effect of Mo-Incorporation in the TiO_2 Lattice: A mechanistic basis for photocatalytic dye degradation. **2014**, *118* (29), 15946–15962, 10.1021/jp5054666.

13. Yu, S.; Liu, B.; Wang, Q.; Gao, Y.; Shi, Y.; Feng, X.; An, X.; Liu, L.; Zhang, J., Ionic Liquid Assisted Chemical Strategy to TiO_2 Hollow Nanocube Assemblies with Surface-Fluorination and Nitridation and High Energy Crystal Facet Exposure for Enhanced Photocatalysis. *ACS applied materials & interfaces* **2014,** *6* (13), 10283-10295, 10.1021/am5016809.

14. Gindri, I. M.; Frizzo, C. P.; Bender, C. R.; Tier, A. Z.; Martins, M. A. P.; Villetti, M. A.; Machado, G.; Rodriguez, L. C.; Rodrigues, D. C., Preparation of TiO_2 nanoparticles coated with ionic liquids: a supramolecular approach. *ACS applied materials & interfaces* **2014,** *6* (14), 11536-11543, 10.1021/am5022107.

15. Łuczak, J.; Paszkiewicz, M.; Krukowska, A.; Malankowska, A.; Zaleska-Medynska, A., Ionic liquids for nano-and microstructures preparation. Part 1: properties and multifunctional role. *Advances in colloid and interface science* **2016,** *230*, 13-28, 10.1016/j.cis.2015.08.006.

16. Paszkiewicz, M.; Łuczak, J.; Lisowski, W.; Patyk, P.; Zaleska-Medynska, A., The ILs-assisted solvothermal synthesis of TiO_2 spheres: The effect of ionic liquids on morphology and photoactivity of TiO_2. *Applied Catalysis B: Environmental* **2016,** *184*, 223-237, 10.1016/j.apcatb.2015.11.019.

17. Kaur, N.; Singh, V., Current status and future challenges in ionic liquids, functionalized ionic liquids and deep eutectic solvent-mediated synthesis of nanostructured TiO_2: a review. *New Journal of Chemistry* **2017,** *41* (8), 2844-2868, 10.1039/C6NJ04073J.

18. Wender, H.; Feil, A. F.; Diaz, L. B.; Ribeiro, C. S.; Machado, G. J.; Migowski, P.; Weibel, D. E.; Dupont, J.; Teixeira, S. R., Self-organized TiO_2 nanotube arrays: synthesis by anodization in an ionic liquid and assessment of photocatalytic properties. *ACS applied materials & interfaces* **2011,** *3* (4), 1359-1365, 10.1021/am200156d.

19. Qi, L.; Yu, J.; Jaroniec, M., Enhanced and suppressed effects of ionic liquid on the photocatalytic activity of TiO_2. *Adsorption* **2013,** *19*, 557-561, 10.1007/s10450-013-9478-7.

20. Marr, P. C.; Marr, A. C., Ionic liquid gel materials: applications in green and sustainable chemistry. *Green Chemistry* **2016,** *18* (1), 105-128, 10.1039/C5GC02277K.

21. Chang, S.-m.; Lee, C.-y., A salt-assisted approach for the pore-size-tailoring of the ionic-liquid-templated TiO_2 photocatalysts exhibiting high activity. *Applied Catalysis B: Environmental* **2013,** *132*, 219-228, 10.1016/j.apcatb.2012.11.026.

22. Lopes, C. W.; Finger, P. H.; Mignoni, M. L.; Emmerich, D. J.; Mendes, F. M. T.; Amorim, S.; Pergher, S. B. C., TiO_2-TON zeolite synthesis using an ionic liquid as a structure-directing agent. *Microporous and Mesoporous Materials* **2015,** *213*, 78-84, 10.1016/j.micromeso.2015.04.014.

23. Yu, N.; Gong, L.; Song, H.; Liu, Y.; Yin, D., Ionic liquid of [Bmim]+ Cl− for the preparation of hierarchical nanostructured rutile titania. *Journal of Solid State Chemistry* **2007,** *180* (2), 799-803, 10.1016/j.jssc.2006.11.008.

24. Gołąbiewska, A.; Paszkiewicz-Gawron, M.; Sadzińska, A.; Lisowski, W.; Grabowska, E.; Zaleska-Medynska, A.; Łuczak, J., Fabrication and photoactivity of ionic liquid–TiO_2 structures for efficient visible-light-induced photocatalytic decomposition of organic pollutants in aqueous phase. *Beilstein Journal of Nanotechnology* **2018,** *9*, 580-590, 10.3762/bjnano.9.54 .

25. Han, C.-C.; Ho, S.-Y.; Lin, Y.-P.; Lai, Y.-C.; Liang, W.-C.; Chen-Yang, Y.-W., Effect of π–π stacking of water miscible ionic liquid template with different cation chain length and content on morphology of mesoporous TiO_2 prepared via sol–gel method and the applications. *Microporous and Mesoporous Materials* **2010,** *131* (1), 217-223, 10.1016/j.micromeso.2009.12.026.

26. Chen, Y.; Li, W.; Wang, J.; Gan, Y.; Liu, L.; Ju, M., Microwave-assisted ionic liquid synthesis of Ti3+ self-doped TiO_2 hollow nanocrystals with enhanced visible-light photoactivity. *Applied Catalysis B: Environmental* **2016,** *191*, 94-105, 10.1016/j.apcatb.2016.03.021.

27. Łuczak, J.; Paszkiewicz-Gawron, M.; Długokęcka, M.; Lisowski, W.; Grabowska, E.; Makurat, S.; Rak, J.; Zaleska-Medynska, A., Visible light photocatalytic activity of ionic liquid-TiO_2 spheres: effect of the ionic liquid's anion structure. *ChemCatChem* **2017,** 9, 4377-4388, 10.1002/cctc.201700861.

28. Kim, S.; Ko, K. C.; Lee, J. Y.; Illas, F., Single oxygen vacancies of (TiO_2) 35 as a prototype reduced nanoparticle: implication for photocatalytic activity. *Physical Chemistry Chemical Physics* **2016,** *18* (34), 23755-23762, 10.1039/C6CP04515D.

29. Ya Jiang; Ying-Jie Zhu, a.; Cheng, G.-F., Synthesis of Bi_2Se_3 Nanosheets by Microwave Heating Using an Ionic Liquid. *Y.jiang, YJ.Zhu, GF.Cheng* **2006**, 6 (9), 2174–2176, 10.1021/cg060219a.

30. Kaper, H.; Sallard, S. b.; Djerdj, I.; Antonietti, M.; Smarsly, B. M., Toward a Low-Temperature Sol–Gel Synthesis of TiO_2 (B) Using Mixtures of Surfactants and Ionic Liquids. *Chemistry of materials* **2010,** *22* (11), 3502-3510, 10.1021/cm100627g.

31. Verma, Y. L.; Tripathi, A. K.; Singh, V. K.; Balo, L.; Gupta, H.; Singh, S. K.; Singh, R. K., Preparation and properties of titania based ionogels synthesized using ionic liquid 1-ethyl-3-methyl imidazolium thiocyanate. *Materials Science and Engineering: B* **2017,** *220*, 37-43, 10.1016/j.mseb.2017.03.010.

32. Jing, L.; Wang, M.; Li, X.; Xiao, R.; Zhao, Y.; Zhang, Y.; Yan, Y.-M.; Wu, Q.; Sun, K., Covalently functionalized TiO_2 with ionic liquid: A high-performance catalyst for photoelectrochemical water oxidation. *Applied Catalysis B: Environmental* **2015,** *166*, 270-276, 10.1016/j.apcatb.2014.11.046.

33. Ravishankar, T. N.; Nagaraju, G.; Dupont, J., Photocatalytic activity of Li-doped TiO_2 nanoparticles: Synthesis via ionic liquid-assisted hydrothermal route. *Materials Research Bulletin* **2016,** *78*, 103-111, 10.1016/j.materresbull.2016.02.017.

34. Liu, H.; Liang, Y.; Hu, H.; Wang, M., Hydrothermal synthesis of mesostructured nanocrystalline TiO_2 in an ionic liquid–water mixture and its photocatalytic performance. *Solid State Sciences* **2009,** *11* (9), 1655-1660, 10.1016/j.solidstatesciences.2009.06.011.

35. Shahi, S. K.; Kaur, N.; Singh, V., Fabrication of phase and morphology controlled pure rutile and rutile/anatase TiO_2 nanostructures in functional ionic liquid/water. *Applied Surface Science* **2016,** *360, Part B*, 953-960, 10.1016/j.apsusc.2015.11.092.

36. Yan, X.; Ohno, T.; Nishijima, K.; Abe, R.; Ohtani, B., Is methylene blue an appropriate substrate for a photocatalytic activity test? A study with visible-light responsive titania. *Chemical Physics Letters* **2006,** *429* (4), 606-610, 10.1016/j.cplett.2006.08.081.

37. Ohtani, B., Photocatalysis A to Z—What we know and what we do not know in a scientific sense. *Journal of Photochemistry and Photobiology C: Photochemistry Reviews* **2010,** *11* (4), 157-178, 10.1016/j.jphotochemrev.2011.02.001.

38. Li, F.-t.; Wang, X.-j.; Zhao, Y.; Liu, J.-x.; Hao, Y.-j.; Liu, R.-h.; Zhao, D.-s., Ionic-liquid-assisted synthesis of high-visible-light-activated N–B–F-tri-doped mesoporous TiO_2 via a microwave route. *Applied Catalysis B: Environmental* **2014,** *144*, 442-453, 10.1016/j.apcatb.2013.07.050.

39. Mirhoseini, F.; Salabat, A., Ionic liquid based microemulsion method for the fabrication of poly (methyl methacrylate)–TiO_2 nanocomposite as a highly efficient visible light photocatalyst. *RSC Advances* **2015,** *5* (17), 12536-12545, 10.1039/C4RA14612C.

40. Alammar, T.; Noei, H.; Wang, Y.; Mudring, A.-V., Mild yet phase-selective preparation of TiO_2 nanoparticles from ionic liquids - a critical study. *Nanoscale* **2013,** *5* (17), 8045-8055, 10.1039/c3nr00824j..

41. Djerdj, I.; Tonejc, A. M., Structural investigations of nanocrystalline TiO_2 samples. *Journal of alloys and compounds* **2006,** *413* (1-2), 159-174, 10.1016/j.jallcom.2005.02.105.

42. Naumkin, A. V.; Kraut-Vass, A.; Gaarenstroom, S. W.; Powell, C. J., NIST X-ray Photoelectron Spectroscopy Database, NIST Standard Reference Database 20, version 4.1, 2012. h ttp. *srdata. nist. gov/xps/(accessed March 25, 2013).*

43. Wu, D.; Long, M.; Cai, W.; Chen, C.; Wu, Y., Low temperature hydrothermal synthesis of N-doped TiO_2 photocatalyst with high visible-light activity. *Journal of Alloys and Compounds* **2010,** *502* (2), 289-294, 10.1016/j.jallcom.2010.04.189.

44. Dolat, D.; Quici, N.; Kusiak-Nejman, E.; Morawski, A. W.; Puma, G. L., One-step, hydrothermal synthesis of nitrogen, carbon co-doped titanium dioxide (N, $CTiO_2$) photocatalysts. Effect of alcohol degree and chain length as carbon dopant precursors on photocatalytic activity and catalyst deactivation. *Applied Catalysis B: Environmental* **2012,** *115*, 81-89, 10.1016/j.apcatb.2011.12.007.

45. Peng, F.; Cai, L.; Huang, L.; Yu, H.; Wang, H., Preparation of nitrogen-doped titanium dioxide with visible-light photocatalytic activity using a facile hydrothermal method. *journal of Physics and Chemistry of Solids* **2008,** *69* (7), 1657-1664, 10.1016/j.jpcs.2007.12.003.